Infrared Photodissociation Spectroscopy of Protonated Acetylene and Its Clusters

G. E. Douberly, A. M. Ricks, B. W. Ticknor, W. C. McKee, P. v. R. Schleyer, and M. A. Duncan*

Department of Chemistry, University of Georgia, Athens, Georgia 30602-2556

Received: November 12, 2007

The protonated acetylene cation, $C_2H_3^+$, (also known as the vinyl cation) and the proton-bound acetylene dimer cation ($C_4H_5^+$) are produced by a pulsed supersonic nozzle/pulsed electrical discharge cluster source. The parent ions are also generated with weakly attached argon "tag" atoms, e.g., $C_2H_3^+$Ar and $C_4H_5^+$Ar. These ions are mass selected in a specially designed reflectron time-of-flight mass spectrometer and studied with infrared laser photodissociation spectroscopy in the 800−3600 cm^{-1} region. Vibrational resonances are detected for both ions in the C−H stretching region. $C_2H_3^+$ has a strong vibrational resonance near 2200 cm^{-1} assigned to the bridged proton stretch of the nonclassical ion, while $C_4H_5^+$ has no such free-proton vibration. Instead, $C_4H_5^+$ has resonances near 1300 cm^{-1}, consistent with a symmetrically shared proton in a di-bridged structure. Although the shared proton structure is not the lowest energy isomer of $C_4H_5^+$, this species is apparently stabilized under the supersonic beam conditions. Larger clusters containing additional acetylene units are also investigated via the elimination of acetylene. These species have new IR bands indicating that rearrangement reactions have taken place to produce core $C_4H_5^+$ ions with the methyl cyclopropane cation structure and/or the protonated cyclobutadiene isomer. Ab initio (MP2) calculations provide structures and predicted spectra consistent with all of these experiments.

Introduction

Hydrocarbon ions known as carbocations are well-known intermediates in organic chemistry,[1,2] and these species have been studied extensively in gas-phase mass spectrometry.[3] Small carbocations are also important in astrophysics and are believed to be abundant in interstellar gas clouds.[4,5] Based on reactivity patterns, dissociation channels, and many theoretical calculations of structures, it is now recognized that carbocations often exhibit multiple isomeric forms that may lie close in energy.[3] The $C_2H_3^+$ ion is a well-studied example of this behavior. Its symmetric bridged configuration, known as protonated acetylene, has a so-called "nonclassical" structure, with nominally five-coordinate carbon atoms. The $HC^+{=}CH_2$ species, known as the vinyl cation, lies close to this in energy with "classical" bonding. This ion and its two structures have been studied extensively with theory.[6−14] The infrared spectroscopy of $C_2H_3^+$ has been investigated in the C−H stretching region,[15] and its pure rotational spectrum has been studied at millimeter and submillimeter wavelengths,[16−18] but there is no previous data for the corresponding proton-bound dimer or the larger clusters of this system. In the present study, a new broadly tunable infrared laser system is employed to probe $C_2H_3^+$ and its protonated dimer using photodissociation spectroscopy and the method of rare gas tagging.[19−23] Larger clusters in this same system are studied via photodissociation and elimination of acetylene molecules. The spectra across a wider range of infrared wavelengths provides new insight into the structure of these prototypical ions.

The classical versus nonclassical structures of protonated acetylene have been investigated extensively over the years with various forms of computational chemistry.[6−14] Although the correct energy ordering for these isomers was unclear in the early work, the consensus of recent theory is that the bridged, nonclassical structure lies about 4 kcal/mol lower in energy than the classical species.[11−14] Infrared spectroscopy for $C_2H_3^+$ in the C−H stretching region has been measured in AC discharges and hollow cathode sources by Oka and co-workers.[15] The spectra of the desired $C_2H_3^+$ ion was separated from many lines of acetylene and other related hydrocarbon ions and neutrals using velocity modulation techniques. Ground vibrational state and C−H excited levels exhibited tunneling splittings with different magnitudes. From this, the structural picture derived for this ion was one with the nonclassical structure, but with a dynamic tunneling motion that exchanged three essentially equivalent hydrogen atoms. A similar picture was derived from the pure rotational spectra in the submillimeter wave region, where the tunneling splittings in the ground vibrational state were documented.[16−18] The ground vibrational state barrier to this tunneling motion was determined at 4−5 kcal/mol. Recent Coulomb explosion imaging (CEI) experiments called into question the structural conclusions of these high-resolution spectra.[24,25] However, ab initio path integral molecular dynamics simulations[13] and the detailed analysis of the full molecular potential surface[14] support the original structural picture derived from the high-resolution spectroscopy. The present experiment employs a pulsed nozzle/pulsed discharge source to make supersonically cooled $C_2H_3^+$ and $C_2H_3^+$Ar ions. Moreover, we use mass-selection to guarantee that only the desired ion is present in the laser interaction region. The broadly tunable infrared OPO laser system now available provides more extensive coverage of the IR spectrum, making it possible to observe vibrations other than the C−H stretches. In particular, we are able to investigate the lower frequency region of the infrared spectrum for the first time. Comparison with the

* To whom correspondence should be addressed. E-mail: maduncan@uga.edu.

10.1021/jp710808e CCC: $40.75
Published on Web 02/12/2008

predictions of theory make it possible to assign the new vibrations observed.

Proton-bound dimer ions have attracted much recent attention.[26−42] In particular, the protonated water dimer has been studied extensively with experiment[27−35] and theory,[34b,36] as have other R−O···H$^+$···O−R′ systems.[37−40] There are virtually no studies of proton-bound dimers of hydrocarbon species like acetylene.[41,42] The infrared spectrum measured here for the protonated acetylene dimer investigates both the C−H stretching region and the lower frequency fingerprint region. Again, by comparison with the predictions of theory, the structure of the proton-bound dimer is revealed.

Experimental Section

The $C_2H_3^+$ and $C_4H_5^+$ ions and their weakly bound argon complexes, $C_2H_3^+Ar$ and $C_4H_5^+Ar$, as well as larger clusters, are produced by a pulsed high voltage discharge in a pulsed supersonic expansion. The gas mixture contains acetylene (0.3%) with 10% H_2, 10% Ar, and a balance of so-called "first-run" neon (70% Ne/30% He). The discharge is produced by a pair of sewing needles (shaft diameter 1 mm) mounted in Teflon blocks on the face plate of a General Valve (Series 9). The two needle tips are adjusted to form a gap with about 1 mm spacing, which is mounted 4−5 mm downstream from the 0.5 mm diameter orifice of the pulsed valve. High voltage is applied to one needle in the form of a 5 μs pulse, generated by a high voltage pulser (DEI model PVX-4140), going from ground to negative 800 V, and the other needle is grounded. The discharge fires in the center of the molecular beam valve pulse of about 250−300 microsecond duration and 20−25 atm backing pressure.

The supersonic expansion produced by the discharge source is collimated by a skimmer and the cations in the resulting molecular beam are measured with a pulsed sampling reflectron time-of-flight mass spectrometer. This instrument is mounted perpendicular to the molecular beam axis in a differentially pumped detection chamber. The operation of this instrument for ion photodissociation spectroscopy has been described previously.[23] The desired ion is mass selected by its flight time with pulsed deflection plates located in the first of two flight tube sections. Photodissociation occurs in the turning region of the reflectron field, where the selected ion is excited with a pulsed infrared optical parametric oscillator/amplifier (OPO/OPA) laser system (Laser Vision) pumped by an injection-seeded Nd:YAG laser (Spectra Physics model PRO-230, equipped with "BeamLok"). The frequency range of 2000−4000 cm^{-1} is obtained using KTP oscillator and KTA amplifier crystals, while the range of 800−2000 cm^{-1} employs difference frequency generation in a $LiInS_2$ or $AgGaSe_2$ crystal. Residual parent ions and any resulting photofragments are mass analyzed by their flight time through a second flight tube section. Infrared spectra are measured by recording the fragment ion signal versus the infrared wavelength with a digital oscilloscope (LeCroy WaveRunner 6051A).

Ab initio calculations are carried out at the MP2(fc) 6-311++G(2p,2d) level, employing either the Gaussian 03W[43] or GAMESS program packages.[44] Selected species were also studied at the MP2(full) aug-cc-pVTZ level to investigate the effects of the different basis set. Vibrational frequencies are scaled for comparison to the experiment by a factor of 0.95.[45] The Supporting Information for this manuscript contains the full details of these calculations, including the structures, energetics, and vibrational frequencies for each of the isomeric structures considered.

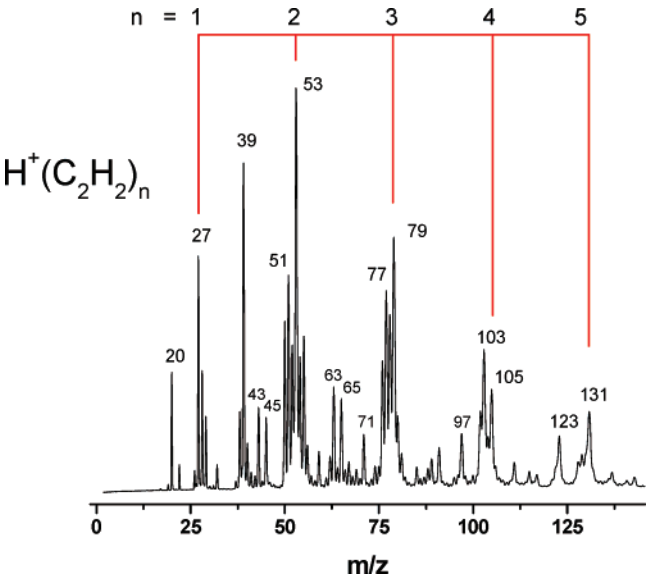

Figure 1. Mass spectrum of the hydrocarbon ions produced by our pulsed-discharge source for the acetylene gas mixture.

Results and Discussion

Figure 1 shows a mass spectrum of the cations and cluster ions produced by our discharge source with the acetylene/hydrogen gas mixture. The conditions and gas mixture were optimized to produce the protonated acetylene ion and its clusters, as opposed to producing the acetylene cation and its clusters without protonation. As shown in the figure, the mass spectrum contains a strong signal at 27 amu, which corresponds to the protonated acetylene cation, and then there is a series of mass peaks spaced by the increment of 26 amu following this that apparently correspond to $H^+(C_2H_2)_n$ cluster ions. In addition to these cluster ions built on protonated acetylene, there are several other common ions that we find in many hydrocarbon plasmas, including mass 39 ($C_3H_3^+$), mass 51 ($C_4H_3^+$), and some of their clusters with acetylene. However, the pure protonated acetylene cluster series is quite prominent, suggesting that "simple" clustering reactions are efficient.

Mass-selected ion beams have extremely low densities, and direct absorption spectroscopy on these ions is not usually feasible. Therefore, ion spectroscopy often is accomplished with resonance-enhanced photodissociation, using the high sensitivity of mass spectrometer detection. However, based on the previous estimates of the thermochemistry for $C_2H_3^+$, dissociation of this ion should require roughly 150 kcal/mol.[6−14] Photodissociation of this ion in the infrared region of the spectrum is not expected to be efficient. We therefore employ the method of rare gas "tagging"[19−23] (also known as rare gas predissociation spectroscopy) to enhance the photodissociation yield, making it possible to obtain spectra in the infrared. In this method, the ion of interest is produced with one or more attached rare gas atoms (typically argon or neon), and then photoexcitation occurs on vibrational resonances via elimination of the weakly bound rare gas atom. It is often the case that such an attached rare gas atom does not perturb the structure or the spectroscopy of the target ion, acting instead to provide a mechanism for measuring its spectroscopy. In the present system, we produce $C_2H_3^+Ar$ and $C_4H_5^+Ar$, and study these species via photodissociation in the argon-loss mass channels. Moreover, we have performed high level ab initio calculations of the bare ions and their argon complexes to investigate the role of the tag atom on the structure and spectroscopy.

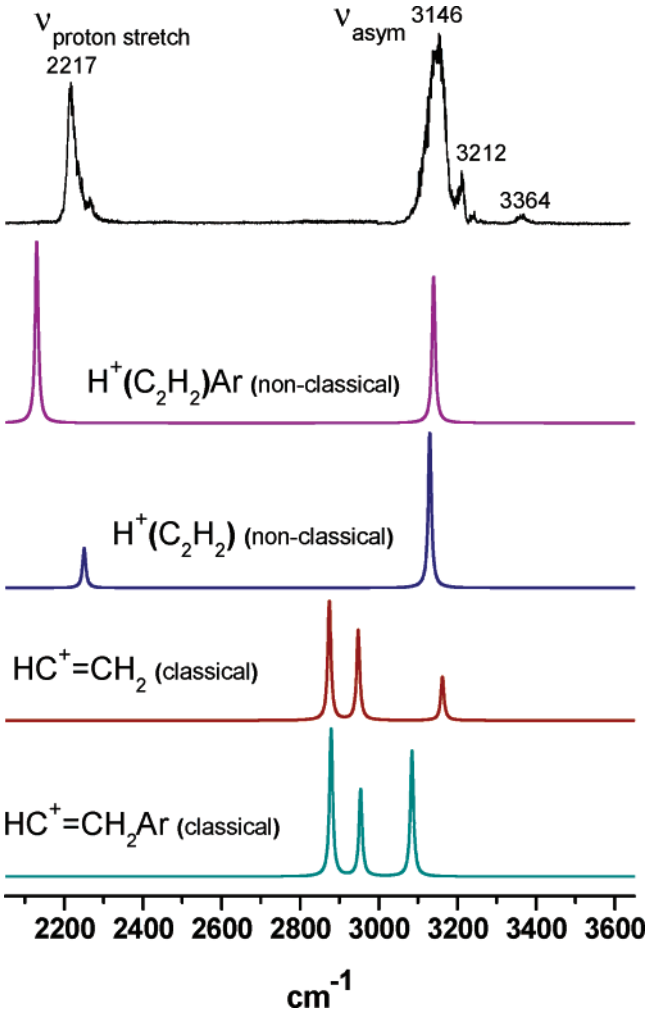

Figure 2. Infrared spectrum for $H^+(C_2H_2)$ in the 2000−3700 cm^{-1} region measured via the argon tagging method. The experimental spectrum is compared to those predicted by theory for the classical and nonclassical structures with and without attached argon. All the theoretical spectra are presented with correct relative IR intensities.

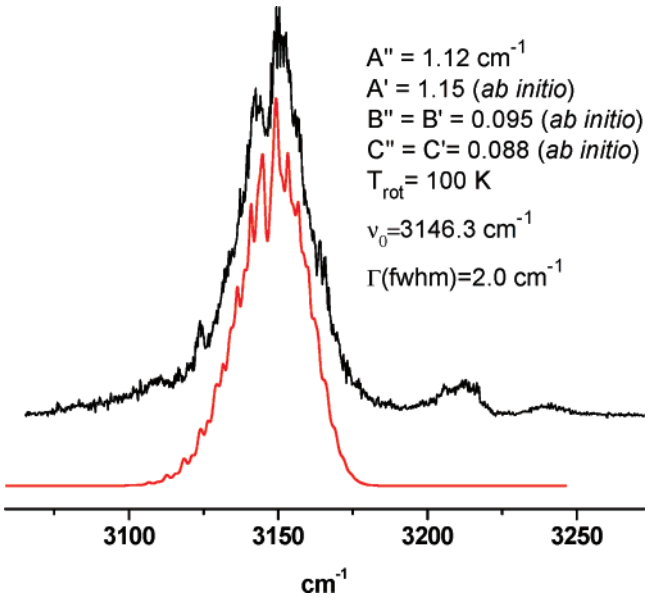

Figure 3. Expanded view of the band measured for the $H^+(C_2H_2)Ar$ complex in the C−H stretching region, showing some partially resolved rotational structure. The experimental spectrum (black) is compared to the rotational contour predicted (red) for an asymmetric top with two equivalent hydrogens (3:1 nuclear spin weighting) and the rotational constants indicated.

$C_2H_3^+$. Figure 2 shows the infrared photodissociation spectrum of $C_2H_3^+Ar$ measured in the argon elimination mass channel. The traces below the experimental spectrum show the spectra predicted by theory for the nonclassical and classical structures of this ion with and without argon tagging. The structures calculated for these ions and their full list of vibrational frequencies are presented in the Supporting Information. The spectrum consists of two main features, including a broad peak centered at 3146 cm^{-1} and another at 2217 cm^{-1}. Both of these have some structure along their edges and weaker satellite peaks/shoulders on their higher energy sides. Because of its position, the 3146 cm^{-1} band is readily associated with the expected asymmetric C−H stretching mode. This is apparently the same band seen by Oka at 3142.2 cm^{-1} for the $C_2H_3^+$ ion at higher resolution and higher temperature in discharge environments.[15] Our spectrum for $C_2H_3^+Ar$ shows that argon tagging has a small, but non-negligible, effect on the position of this band. However, Oka's spectra was fully rotationally resolved and ours is not. Therefore, our frequency assignment has some uncertainty because of our choice for the center of this broad band. It is understandable that argon would not have a major effect on the asymmetric C−H stretch in the expected proton-bridged structure, because it is bound at the proton site on the C_2 axis, which is remote from the C−H groups. As noted by Oka, this C−H stretching frequency also occurs quite close to that in the acetylene molecule (3136 cm^{-1}).[46]

The lower traces of Figure 2 show the vibrational structure predicted by theory in the C−H stretching region for the classical versus nonclassical structures of $C_2H_3^+$, with and without argon tagging. The details of the structures computed for these complexes and the vibrational frequencies derived from them are given in the Supporting Information, and their energetics are given in Table 1. These details are essentially unchanged when the computations are carried out at the MP2-(fc) 6-311++G(2p,2d) level (shown) or at the MP2(full) aug-cc-pVTZ level. In the nonclassical proton-bridged structure, the argon is bound on the proton on the C_2 axis. In the classical structure, the argon is bound on the single C−H group, also on the C_2 symmetry axis for this system. The nonclassical structure has one main feature predicted in the C−H stretching region, consistent with the experiment, while the classical structure has three separate C−H stretches spread out over a broader frequency range. These three frequencies are associated with the inequivalent CH and CH_2 groups in this structure; the latter has symmetric and asymmetric stretches. According to theory, argon has only a minor effect on the C−H stretch in the nonclassical structure. The scaled value of this frequency is predicted at 3120 cm^{-1} for the isolated $C_2H_3^+$ molecule and at 3134 cm^{-1} for the argon tagged species. The argon shifts in the bands for the classical structure are predicted to be greater, but there are still three bands spread out over the 2800−3200 cm^{-1} region. Because of his limited wavelength coverage, Oka could only probe the region near 3100 cm^{-1}. However, because of our broader wavelength coverage, we can confirm that the band seen by Oka is the only strong one in this region of the spectrum. It is clear then that the pattern of bands here agrees nicely with the one expected for the nonclassical structure and is not consistent with the classical structure.

To examine the C−H stretching region more closely, we have simulated the rotational contour expected for the asymmetric stretch of the $C_2H_3^+Ar$ complex in its nonclassical structure

TABLE 1: Isomers of the $C_2H_3^+$ and $C_2H_3^+$Ar Ions, Their Relative Energies, and Their Vibrational Frequencies (Unscaled) Calculated at the MP2(fc) 6-311++G(2d,2p) Level of Theory Using GAMESS

isomer	total energy (Hartrees)	relative energy (kcal/mol)	vibrational frequencies (cm^{-1})
$C_2H_3^+$ nonclassical	−77.3795656	+0.0	573.7(0), 693.8(25.9), 759.7(111.3), 921(47), 1316(8.8), 1923(5.7), 368.8(102.5), 3294.1(399.4), 3397.4(0.1)
$C_2H_3^+$ classical	−77.3682369	+7.1	−67.4(42.3), 661.3(24.6), 812.8(134), 110.4(0.9), 1182.4(84.5), 1765.7(85.4), 3025.1(307.2), 3102.3(232.4), 3327.8(112)
$C_2H_3^+$Ar nonclassical	−604.3626211	+0.0	89.8(8.6), 104.6(42.7), 286.8(35.5), 577.2(0), 688.1(22.6), 761.4(106.9), 915.3(30.6), 1309.7(12.3), 1928.6(14.4), 2241.9(467.4), 3304.3(376.9), 3407.1(0.8)
$C_2H_3^+$Ar classical	−604.3501212	+7.8	20.1(7.3), 79.5(1.6), 89(35.5), 117.3(33), 709.3(5.9), 822.8(133.1), 1139.8(0.1), 1186.5(75.6), 1760.9(140.3), 3029.8(380.3), 3108.7(223.1), 3246.2(324.1)

(perpendicular-type band, with appropriate nuclear spin weighting). Figure 3 shows an expanded view of the spectrum and this simulation. Although our spectrum is by no means high resolution, several of the rough features of the contour do match those in the simulation, providing consistency with the nonclassical structure and the position of the argon. If the argon were attached on one of the terminal C−H positions rather than on the bridged proton, the contour would be much more narrow and would have a different structure. This contour also allows us to estimate the temperature of these ions, which we find to be about 100 K. By matching the contour with the simulation, we are able to determine the position for the band origin, i.e., 3146 cm^{-1}. We are also able to determine that the weak higher frequency bands at 3212 and 3364 are not caused by rotational structure, as these do not appear in the rotational simulation. A weak vibrational band is predicted at higher frequency for both the tagged and untagged species, and this could explain at least one of these features. Another possibility is a combination band involving an argon stretch vibration.

The most interesting aspect of this spectrum is the strong vibrational band at 2217 cm^{-1}. There are no previous measurements for $C_2H_3^+$ in this frequency region because the IR lasers required were not available. As shown in Figure 1, the classical structure of the vinyl cation has no vibrations anywhere close to this frequency. Instead, an intense vibration is expected here only for the nonclassical proton-bridged structure, associated with the stretch of the proton perpendicular to the acetylene molecular axis. Because the charge is localized here, there is a dramatic effect on the dipole during vibrational motion, and this band is expected to be quite intense, as we observe. We therefore assign this band to the proton stretching vibration. To our knowledge, this is the first observation of such a π-bridging proton vibration for any gas-phase ion.

The position of the proton stretching mode is reasonably well predicted by our computations, especially if the argon is included. However, unlike the C−H stretch, the presence of argon has a significant effect on the proton stretch. The frequency of this vibration also varies more with the basis set and level of theory employed. According to our computations at the MP2(fc) 6-311++G(2p,2d) level, this vibration is shifted 127 cm^{-1} further to the red in the tagged complex than it is in the isolated $C_2H_3^+$ ion, and the IR intensity increases by a factor of 4. In the computed structure, the argon is predicted to be bound directly to the proton, and therefore a strong perturbation on this mode induced by the argon is understandable. Using our measured value for the tagged complex and our computed value for the argon-induced shift, we can predict that the free $C_2H_3^+$ ion will have a proton stretch at about 2340−2350 cm^{-1}. This value can be compared to that from previous theoretical work by Lindh et al., which computed a value of 2385 cm^{-1}.[12] More recently, Bowman and co-workers performed an extensive analysis of the potential in this system, deriving a value of 2358 cm^{-1} for this vibration through a potential fit,[14] which is in excellent agreement with our estimated value.

The proton stretch in this acetylene system can be compared to those in other ion−molecule complexes studied recently. The asymmetric stretch of hydronium occurs near 3500 cm^{-1},[47] but in this system the charge is more delocalized. Dopfer and coworkers,[48] as well as our group,[49] have studied the free-proton stretch in protonated carbon dioxide, which occurs at 2700 cm^{-1} for the argon-tagged complex. Argon has a similar dramatic effect on this system, as this same vibration without the argon is calculated to occur at 3400 cm^{-1}. In our own recent work for the protonated acetone complex, the proton stretch occurs at 3377 cm^{-1} with argon attached, compared to the frequency of 3450/3508 cm^{-1} calculated with/without argon.[50] We have also computed the proton stretch vibration for the nonclassical structure of protonated ethylene, which is predicted at 2070/2127 cm^{-1} with/without the argon.[51] It is clear that argon has a non-negligible effect when it binds at the proton site, as it does in all of these systems. Argon shifts the proton stretch to lower frequencies, closer to where proton vibrations for bridged dimers are found (see below), consistent with its role as a weakly interacting proton sharer. It is also apparent that the proton stretch vibration occurs at much lower frequencies for the acetylene and ethylene systems, when the proton interacts with a double or triple-bonded π system, than it does when the proton is bound to a lone-pair in an oxygen-containing molecule. There is no simple correlation with the proton binding energy, as CO_2 has a *lower* proton affinity than acetylene (129.1 vs 153.3 kcal/mol)[52] but a higher proton stretch frequency. However, the oxygen-containing molecules are heavier on average, and it may be that the proton stretch in these systems is more of a local oscillator than it is in the lighter molecules, resulting in a higher vibrational frequency.

It is interesting to consider whether the frequency of this proton stretch has any implications for the *dynamical* structure of $C_2H_3^+$. As noted above, the hydrogens in this system can exchange via tunneling, and the implications of this for the vibration−rotation spectrum have been investigated and discussed thoroughly. Indeed, tunneling splittings have been observed in the high-resolution spectra of Oka[15] and in the millimeter wave spectra.[16−18] However, questions remain about the subtle details of the ground state structure. The global

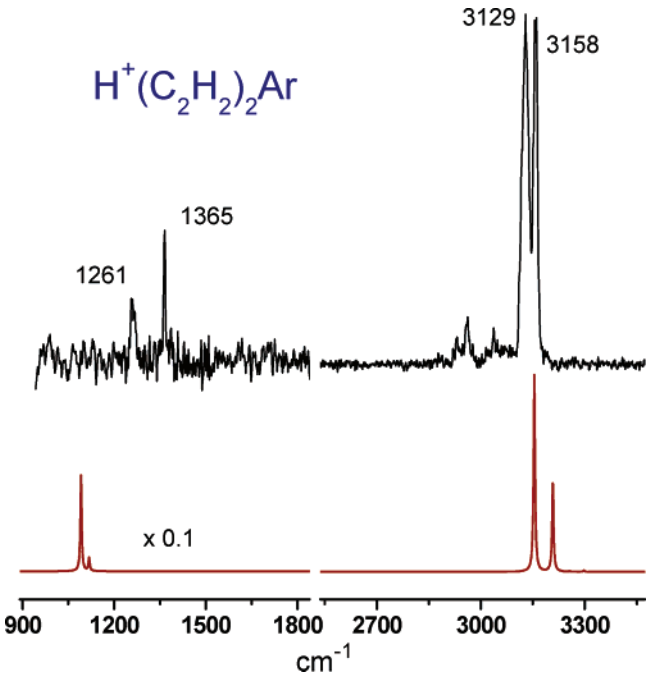

Figure 4. Infrared spectrum measured for $C_4H_5^+Ar$ in the 1000 to 3700 cm^{-1} region compared to the predictions of theory(MP2(fc) 6-311++G(2d,2p) level) for the proton-bound acetylene dimer structure.

minimum energy configuration derived by theory is now generally accepted to be the nonclassical structure with the proton in a symmetric bridging position and the acetylene in a linear configuration. The infrared spectrum of Oka and the millimeter wave spectrum were both interpreted to arise from such a ground state, and ab initio path integral molecular dynamics simulations[13] and the detailed analysis of the full molecular potential surface[14] all support this structure. Our frequency for the proton stretch vibration in the argon complex, and its estimated value for the free molecule, fall almost exactly where this vibration is predicted for this symmetric proton-bridged structure. Our resolution is not great enough to resolve any tunneling splittings. However, the Coulomb explosion imaging (CEI) experiments have been analyzed in terms of a fluxional structure, with a trans-bent acetylene moiety and a proton undergoing an orbiting motion about the acetylene waist.[24,25] Asymmetric configurations were judged to become more important at elevated temperature. As noted above, our temperature is believed to be about 100 K. However, while our spectrum is consistent with the symmetric bridged ground state, it is not clear that we can exclude the asymmetric configurations proposed by the CEI experiments, as these may also have proton stretching in the same frequency region. This possibility should be investigated more carefully in future dynamical simulations.

$C_4H_5^+$. Figure 4 shows the infrared spectrum recorded for the ion $C_4H_5^+Ar$. Because the mass spectrum in Figure 1 contains species of the form $H^+(C_2H_2)_n$, we expect that $C_4H_5^+$ and $C_4H_5^+Ar$ represent the proton-bridged dimer of acetylene. The spectrum has an intense doublet at 3129/3158 cm^{-1}, which is very close to the C−H band in the protonated monomer at 3146 cm^{-1}. There are also some weaker features just to the red of the doublet and a pair of bands in the lower frequency region at 1261 and 1365 cm^{-1}. The two bands in the C−H stretching region are much sharper than the single one in the $C_2H_3^+$ spectrum, consistent with the smaller rotational constant and tighter contour expected for the heavier ion. The most significant difference between this spectrum and that of $C_2H_3^+$ is that there is no free proton stretch near 2200 cm^{-1}. This ion therefore has the proton enclosed, as we expect for the proton-bridged dimer, or else it has rearranged into another isomeric structure that has no proton in a π-bridging position. To explore these alternatives, we have performed ab initio computations on the structures and spectra of several isomeric variants of $C_4H_5^+$ and their argon-tagged analogues. The results of these computations are presented in the Supporting Information and in Table 2. Where they overlap, our calculations are completely consistent with those of Cunje and co-workers.[53]

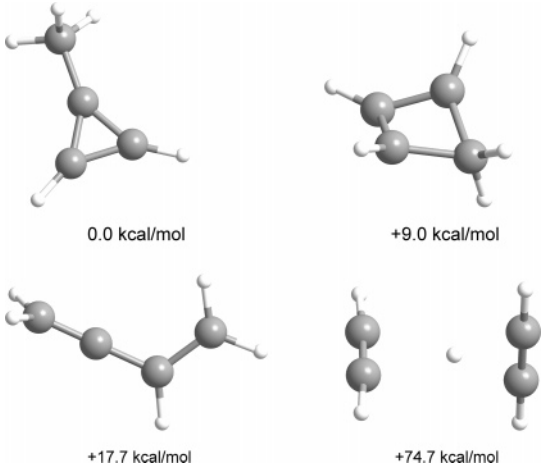

Figure 5. Structures calculated for the different isomers of $C_4H_5^+$: (a) the methyl cyclopropane cation, (b) protonated cyclobutadiene, (c) the allyl-type chain, and d) the proton-bound acetylene dimer.

TABLE 2: Isomers of $C_4H_5^+$ and Their Relative Energies, Calculated at the MP2(fc) 6-311++G(2d,2p) Level of Theory Using GAMESS

isomer	total energy (Hartrees)	relative energy (kcal/mol)
$C_4H_5^+$ methyl cyclopropane	−154.6570880	0.0
$C_4H_5^+$ protonated cyclobutadiene	−154.6426901	+9.0
$C_4H_5^+$ allyl chain	−154.6288478	+17.7
$C_4H_5^+$ proton bound acetylene dimer	−154.5384998	+74.7

As shown in Table 2, the proton-bridged acetylene dimer is by no means the lowest energy structure for $C_4H_5^+$. Instead, several other isomers are expected to lie at lower energy on an absolute stability scale, including the methyl cyclopropane cation, protonated cyclobutadiene and a $(H_2C-CH-C)^+=CH_2$ chain structure with an allyl-like moiety delocalizing the charge near one end. To determine whether any of these other isomers are indeed present, we have calculated their structures and spectra, which are presented in Figures 5 and 6. More details of these computations, including the specific structural parameters computed with and without argon, are provided in the Supporting Information. As shown in Figure 6, none of these isomers other than the proton-bridged dimer has a strong two-band pattern in the C−H stretching region, but rather they all have bands at much lower frequencies than those measured. Also, none of the other isomers has a simple pattern below 1500 cm^{-1} with one or two strong bands. The only isomer of $C_4H_5^+$ whose spectrum matches these qualitative features that we measure is the proton-bridged acetylene dimer. Even though this is a high-energy structure, it is apparently stabilized against rearrangement in our experiment by the rapid cooling in the supersonic expansion and by a barrier in the coordinate that leads to rearrangement. The spectrum predicted by theory for this proton-bridged isomer is shown in Figure 4, where it is plotted below the experimental spectrum. As shown, the major

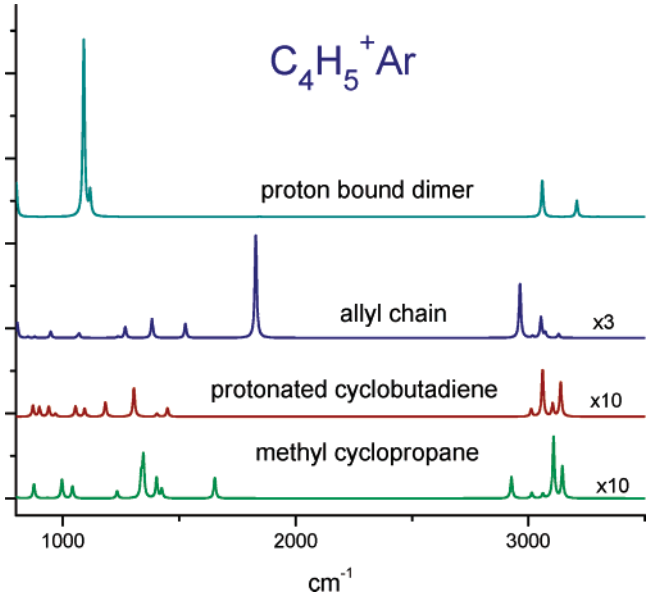

Figure 6. Infrared spectra simulated for the different isomers of $C_4H_5^+$-Ar using the IR band positions and intensities calculated at the MP2-(fc) 6-311++G(2d,2p) level. Frequencies were scaled by a factor of 0.95. All spectra are presented with correct relative IR intensities.

qualitative features of the spectrum are reproduced, but minor bands near 2900−3000 cm^{-1} are not predicted and the doublet at 1261/1365 is also not matched exactly by the theory.

The structure calculated for the proton-bound dimer is one with a near-symmetrically shared proton having the two acetylenes at right angles to each other. The symmetry is nearly D_{2d}, except that the proton is more closely associated with one acetylene than it is with the other (1.279 vs 1.714 Å) at its equilibrium (r_e) position. This structure is consistent with that computed previously by Grabowski et al.[42] The asymmetric proton-binding structure suggests that the potential in the proton-acetylene coordinate has a double minimum. However, an analysis of this potential (see Supporting Information) indicates that the central barrier is only about 15 cm^{-1} above the minima, and therefore its zero-point energy should place the proton above this barrier in the symmetric position. Without the zero-point averaging, there are two strong IR-active vibrations in the C−H stretching region that have significant intensity. These are asymmetric stretches on the two acetylenes, one which is close to the proton and one that is away from it. In the real molecule with zero-point averaging, these modes are degenerate. An out-of-phase symmetric stretch on the two acetylenes is also IR active, but this has very low intensity. In the tagged complex, argon attaches to one of the C−H groups of acetylene, breaking the symmetry of the complex and splitting the asymmetric stretches. The vibration on the acetylene attached to argon is strongly red-shifted by about 120 cm^{-1}, and the one remote from the argon is hardly shifted at all. As shown in the spectrum, we observe these two C−H stretching bands with a spacing and relative intensity in good agreement with the predictions of theory. This confirms not only that two acetylene units are present, but except for the argon, they are essentially equivalent in the structure.

The only other IR-active mode expected above 1000 cm^{-1} is the shared proton stretching motion. We find that the frequency of this vibration is quite sensitive to the basis set employed. At the MP2(fc) 6-311++G(2d,2p) level, the free molecule has a single band predicted at 1009 cm^{-1}, whereas this vibration is at 1212 cm^{-1} at the MP2(full) aug-cc-pVTZ level. However, we find that argon tagging again breaks the symmetry of the complex, and this vibration becomes a doublet predicted at 1091/1118 cm^{-1} at the MP2(fc) 6-311++G(2d,-2p) level. Unfortunately, we were unable to get the calculations to converge at the MP2(full) aug-cc-pVTZ level for the argon complex. As shown in the spectrum, we observe a doublet at 1261/1365 cm^{-1}, which is significantly higher than the values predicted with the smaller basis set. The less-than-perfect agreement between theory and experiment here is not too surprising. Our calculations necessarily derive the proton vibrational frequency for the complex in its asymmetric position at the bottom of the potential well, even though we recognize that the zero-point of this vibration will actually place the proton in a symmetric configuration. This will undoubtedly have a significant effect on the vibrational frequency. Additionally, it is also possible that the frequency of the shared proton vibration is perturbed via Fermi resonance with other low-frequency vibrations. As shown in our computations, the fundamentals of the cis- and trans-bending vibrations on the acetylene units in this complex fall in the frequency range of 600−700 cm^{-1}. Overtones and various combinations of these vibrations would fall in the same frequency region as the fundamental of the shared proton stretch, providing other opportunities for vibrational complexity. The shared proton vibration in this system definitely needs to be investigated with more sophisticated theoretical methods than those employed here.

Shared proton vibrations have been a topic of ongoing interest for the last several years. The IR spectra of these species have been reported for superacid matrix samples,[35,37] but more detailed investigations have been reported for mass-selected ions in the gas phase using free electron lasers[31,32,38,39] or new OPO laser systems[33,34,40] to access the fingerprint region of the IR. In various studies of the protonated water dimer, shared proton stretching vibrations have been measured in the region near 1100 cm^{-1}.[31−35] Initial experiments employing free electron lasers produced broad spectra with complex structure that was sensitive to the laser power employed in multiphoton processes.[31,32] However, more recent studies in the Johnson lab employed rare gas tagging experiments and low laser powers, making it possible to observe spectra more like the one-photon absorption spectrum.[33,34] In these systems, simpler spectra with fewer bands were observed. However, the multiplet structure measured in the spectrum could not be reproduced with harmonic vibrational fundamentals, but rather appeared to be the result of Fermi resonances or other perturbations.[33,34,36] Johnson and co-workers have extended the same methodology to study a variety of R−O···H^+···O−R′ systems with a range of proton affinity differences between R and R′ species.[40] When there is a large proton affinity difference, the proton may become localized and its frequency tends toward much higher values, even approaching the free-proton stretching region seen here for our monomer species. However, for many symmetric systems (i.e., R═R′), the proton stretch was observed in the 1000−1200 cm^{-1} frequency range. Our research group has recently measured the shared proton vibration in the $H^+(CO_2)_2$ and H^+(acetone)$_2$ systems, and the vibrations for these species are found near 900 cm^{-1}.[49,50]

It is understandable that the proton-shared dimer detected here might be formed initially, but it is not clear how this structure can survive when $C_4H_5^+$ has other more stable structures (see Figure 5). Apparently, there must be substantial barriers on the potential surface that limit the rearrangement(s) of this ion. To explore this aspect of the $C_4H_5^+$ system, we have investigated its potential energy surface to attempt to identify barriers, if any, on this surface. Figure 7 shows the results of these

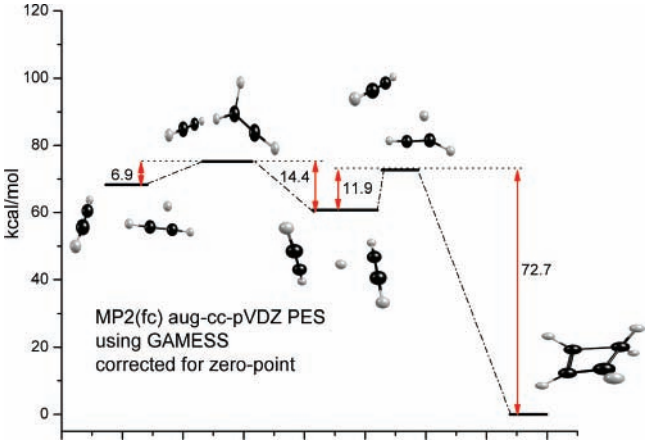

Figure 7. Schematic diagram of the reaction coordinate for $C_4H_5^+$, showing the barriers and relative energies of different possible reaction products.

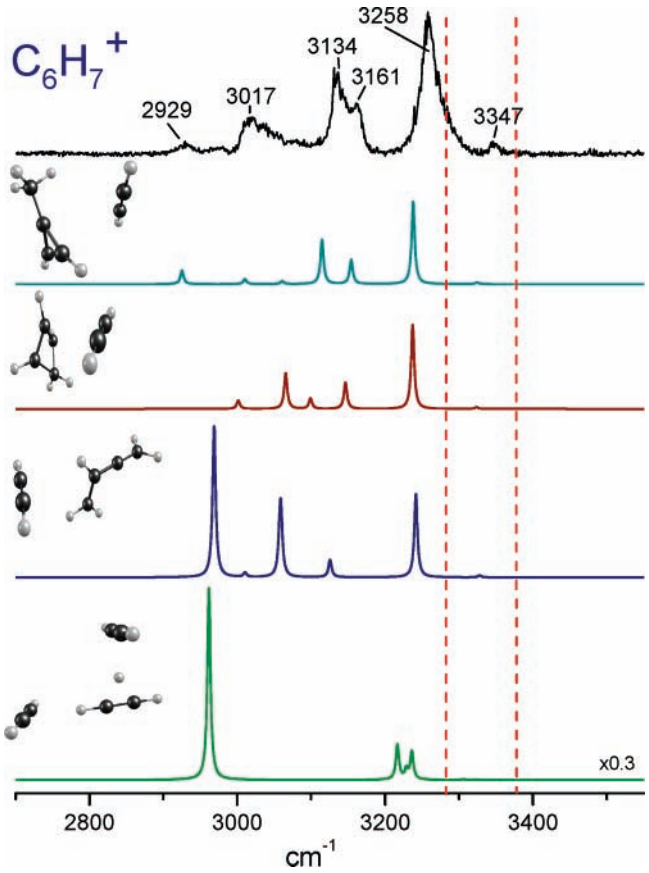

Figure 8. Infrared spectrum measured for the $C_6H_7^+$ ion (black) compared to the spectra predicted by theory for different isomeric clusters of this ion (from MP2(fc) 6-311++G(2d,2p) computations with 0.95 scaling). All the theoretical spectra are presented with correct relative IR intensities. The top trace from theory (cyan) shows the spectrum predicted for the acetylene complex of the methyl cyclopropane cation. The next trace (wine) shows that for the acetylene complex of the protonated cyclobutadiene ion. The third trace (blue) shows the spectrum for the acetylene complex of the allyl-type chain isomer, while the last trace (green) shows the spectrum for the acetylene complex of the proton-shared acetylene dimer. The latter spectrum is scaled downward in absolute intensity because the proton stretch band is so intense.

computations. The proton in the initial $C_4H_5^+$ complex is unsymmetrically sandwiched between two perpendicular acetylenes, with C_{2v} rather than D_{2d} symmetry. Coordinate displacement varies the energy gradually, showing that the proton and its acetylene ligands are quite mobile. Two pathways, both involving C_s symmetry transition structures, are identified (Figure 7). One of these, shown on the left side of the figure, is unproductive, and only leads, over a 14.4 kcal/mol barrier, to a 6.9 kcal/mol higher energy $C_4H_5^+$ complex with a C_2H_2 attached to an end, rather than to the bridged H of a nonclassical vinyl cation. The second pathway, shown on the right of Figure 7, is productive as it leads to the much more stable family of carbon-bound $C_4H_5^+$ isomers (see Figure 5). In effect, the bridged proton in the $C_4H_5^+$ sandwich complex moves to one side to allow attachment of the second C_2H_2 to the exposed carbon. Although not detected in the present experiments, the pathway "downhill" from this achiral C_s $C_4H_5^+$ transition state leads eventually to chiral (extended allyl) products and must involve a ridge-valley inflection point.[54] The final achiral products form subsequently. It is remarkable that the modest barrier along this path (11.4 kcal/mol at MP2(fc)aug-cc-pVDZ) is not overcome under the experimental conditions. The final temperature of the experiment after the supersonic expansion may be near 100 K, at which kT is only about 0.2 kcal/mol. However, higher temperatures are almost certainly present in the early stages of cluster growth in the discharge. In related work, we attempted to observe the corresponding proton-shared *ethylene* dimer, $C_4H_9^+$. However, rearrangement in that system was extremely facile, producing the global minimum $C_4H_9^+$ structure of the tertiary butyl cation.[55]

Larger Clusters. To further examine the nature of proton accommodation in these acetylene-based systems, we have also measured the infrared photodissociation spectra for the $C_6H_7^+$ and $C_8H_9^+$ ions. As shown in Figure 1, these ions are the next two members in the $H^+(C_2H_2)_n$ series in the mass spectrum. Argon tagging was not effective for these larger species, but we found that their photodissociation was efficient in the mass channel corresponding to the loss of acetylene in the C−H stretching region. Unfortunately, these larger ions did not photodissociate at lower energies, and so we could not investigate the free-proton stretch region (near 2200 cm^{-1}) or the shared proton stretch (near 1200−1300 cm^{-1}). The lack of photodissociation at lower energy is consistent with the binding energy for the excess acetylene to these species that we compute (2100−2800 cm^{-1}). The spectrum in the 2800−3500 cm^{-1} region for the $C_6H_7^+$ ion is shown in Figure 7, where it is compared to spectra predicted by theory for various isomeric structures. Both of the spectra for $C_6H_7^+$ and $C_8H_9^+$ (not shown) are quite similar, with a relatively sharp and most intense band near 3260 cm^{-1}, a doublet near 3130/3160 cm^{-1}, and weaker broad bands near 2900 and 3020 cm^{-1}. The doublet near 3130/3160 cm^{-1} corresponds closely to that seen in the proton-shared dimer spectrum at 3129/3158 cm^{-1}. However, the strong feature near 3260 cm^{-1} and the broad bands at lower energy do not appear in either of the spectra for the protonated monomer or dimer.

Because the $C_6H_7^+$ species loses C_2H_2 upon IR excitation, its structure can be viewed as an acetylene-solvated $C_4H_5^+$ unit. We have therefore employed calculations to investigate the isomers of $C_4H_5^+$ discussed above, but now with an extra attached acetylene unit. The IR spectra predicted for these isomers are shown in Figure 7. The lower trace from theory (green) shows the spectrum predicted for the proton-shared acetylene dimer with an additional attached acetylene. This structure would be expected for $C_6H_7^+$ if the dimer structure found above for $C_4H_5^+$ adds an additional acetylene unit in a "simple" solvation process. The spectrum predicted for this structure is much like that of $C_4H_5^+$Ar presented above in Figure

4 in the C−H stretching region, where a doublet is found, but the position of the doublet is predicted to be at higher frequency here. However, because the extra acetylene is bound via a C−H group pointing into its π cloud, there is also a weak hydrogen bond in this structure for $C_6H_7^+$. This leads to a red-shifted C−H stretch that gains extra oscillator strength, and an intense band is predicted near 2960 cm^{-1}. The experimental spectrum for both $C_6H_7^+$ and $C_8H_9^+$ contain a doublet band near 3130/3160 cm^{-1}, whose position is almost exactly the same as that for the $C_4H_5^+Ar$ ion, but this is further to the red than the doublet predicted for the acetylene-solvated proton-shared dimer structure. Also, the broad band near 3020 cm^{-1} is somewhat close to the position predicted for the C−H hydrogen bond. We therefore cannot rule out that a small amount of these ions do represent simple solvation products of $C_4H_5^+$ in the proton-shared dimer structure. However, this kind of structure does not predict any vibrational bands near 3260 cm^{-1}, where the experimental spectra have their strongest feature. Therefore, additional structures must be considered.

To determine what other structures are represented in the larger ions, we have investigated other possible acetylene clustering products including the more stable isomers noted above for $C_4H_5^+$ (see Supporting Information). The upper trace in Figure 7 (cyan) shows the spectrum predicted by theory for a $C_4H_5^+(C_2H_2)$ unit in which the $C_4H_5^+$ core has the methyl cyclopropane cation structure. The second trace (wine) shows the spectrum predicted for $C_4H_5^+(C_2H_2)$ when the $C_4H_5^+$ core has the protonated cyclobutadiene structure. Finally, the third theory trace shows the spectrum predicted for $C_4H_5^+(C_2H_2)$ when the core has the allyl-type chain structure. As shown in the figure, all of these so-called "reacted" structures give rise to a strong band near 3250 cm^{-1} (assigned to the asymmetric stretch of the external acetylene), where the strongest band in the spectrum is seen. Each also has medium intensity bands in the 3000−3150 cm^{-1} region, where weaker bands are measured, and a weak band at 3350 cm^{-1}. However, the allyl chain isomer has a strong band predicted near 2970 cm^{-1} that corresponds to only a broad weak band in the experimental spectrum. Although we cannot rule out a minor contribution from this isomer, it also does not seem to be the major component present. The remaining two theoretical spectra both have peaks in relatively good agreement with the experiment. The top theory trace, which is the one for the acetylene complex of the methyl cyclopropane cation, has almost perfect agreement with the experimental spectrum. This spectrum looks essentially the same as that predicted for this same isomer without the extra acetylene (see Figure 6, bottom trace) except for the strong 3250 cm^{-1} band and the weak 3350 cm^{-1} band. It is therefore tempting to conclude that this structure is the only one present. This is possible, but considering the uncertainties in the theory, it is not possible to completely eliminate the protonated cyclobutadiene structure. We therefore conclude that these spectra for $C_6H_7^+$ and $C_8H_9^+$ represent $C_4H_5^+$ ions that have rearranged to either the methyl cyclopropane cation or the protonated cyclobutadiene structures, each solvated with one or two extra acetylenes. This is satisfying, because these two structures represent the lowest energy isomers for $C_4H_5^+$. Although these isomers of $C_4H_5^+$ have been suggested previously by theory,[53] this is the first observation of their infrared spectra. In related chemistry, we have previously also seen the formation of cyclobutadiene from acetylene when four or more acetylene molecules were attached to the nickel cation.[56]

It is also worth mentioning that the $C_8H_9^+$ spectrum could conceivably represent a protonated benzene structure solvated with one excess acetylene. El-Shall and co-workers have reported the formation of the benzene cation from acetylene excited with energetic electron impact ionization.[57] However, we have calculated this spectrum (see Supporting Information), and we have also measured the protonated benzene spectrum made directly from a benzene precursor.[58] The main features of that spectrum do not match the ones measured here. Therefore, $C_8H_9^+$ in this experiment most likely represents the same core ion structure(s) seen for $C_6H_7^+$, but solvated with one extra acetylene.

It should be noted that our photodissociation mode of detection introduces a possible source of bias in these spectra. For example, it may be true that some bare $C_4H_5^+$ ions do rearrange to the more stable protonated cyclobutadiene or methyl cyclopropane structures. If they are internally warm following this energy-releasing process, then these ions may not attach argon efficiently, and they would not be detected in our experiment on $C_4H_5^+Ar$. According to our computations, argon binds much more weakly ($D_e = 400-600$ cm^{-1}) than acetylene ($D_e = 2100-2800$ cm^{-1}) to these $C_4H_5^+$ ions, and it should attach more effectively to cold ions. However, reacted ions with internal energy could conceivably still attach a stronger-binding acetylene molecule. This would lead to a bias for unreacted species with argon tagging but allow detection of reacted species with attached acetylene. This may explain to some degree why we see only unreacted $C_4H_5^+$ with argon tagging, but reacted isomers of this ion with acetylene elimination. Unfortunately, we only detect the ions at any given mass that have the required leaving group for photodissociation, and we are only able to speculate about what cluster growth processes have produced those ions. However, at each cluster mass that we study, we find that the photodissociation processes are relatively efficient. The spectra that we measure are therefore expected to represent the major population of ions at that mass, regardless of how they were formed.

Conclusions

New infrared spectroscopy measurements are reported for the protonated acetylene cation and its clusters of the nominal form $H^+(C_2H_2)_n$ using mass-selected photodissociation. The small clusters are studied with argon-tagging methods, while the larger species are detected via the photoinduced elimination of acetylene. The spectrum for the $C_2H_3^+$ species is found to be completely consistent with the nonclassical proton-bridged structure. The C−H stretching region in this ion, which is detected with argon-tagging photodissociation spectroscopy, matches well with that reported previously by Oka and co-workers with higher resolution direct absorption measurements. The detection of the bridged proton stretching mode near 2200 cm^{-1} confirms the nonclassical structure and represents the first report of the proton stretching mode in a π-bridged complex.

The spectrum of $C_4H_5^+Ar$ is assigned to the proton-bridged acetylene dimer, providing the first spectroscopic observation of a proton shared between the two π systems of unsaturated hydrocarbons. The shared-proton stretching modes are observed in the 1200−1300 cm^{-1} region. Although there are several lower energy isomers for $C_4H_5^+$, the nonclassical structure of protonated acetylene survives in the bridged dimer, apparently because there are barriers to rearrangement and the cold supersonic expansion conditions inhibit their passage. It is also interesting that the shared proton stretching vibration in this π-bridging system occurs at a frequency quite close to that in the protonated water dimer and other symmetrically shared

proton systems. The specific frequency of the shared proton vibration should depend on the proton binding energy and the detailed shape of the potential in the proton coordinate. We anticipate additional insight as more sophisticated theoretical methods are brought to bear on these fascinating shared-proton interactions.

The IR spectra of larger protonated clusters based on these acetylene systems have also been measured via elimination of acetylene units. These clusters exhibit more complex spectra and are not consistent with "simple" addition of multiple acetylene molecules to the same monomer and dimer units detected individually. Instead, it appears that activation barriers can be traversed more readily in these systems, allowing rearrangements to more stable configurations. The IR chromophores in both $C_6H_7^+$ and $C_8H_9^+$ appear to have significant isomeric contributions from ions based on the core $C_4H_5^+$ moiety with the methyl cyclopropane or protonated cyclobutadiene structures. These core ions are the two lowest energy isomers for $C_4H_5^+$, and the present data provides the first experimental evidence for these structures. The presence of more reaction products in larger clusters is understandable and is expected to vary considerably in efficiency depending on the ion source conditions (initial temperature and cooling rate). Other more complex structures are conceivable from these same starting materials and the IR methods used here may also be able to detect such species in the future.

Acknowledgment. We gratefully acknowledge support for this work from the National Science Foundation (Duncan Grant No. CHE-0551202 and Schleyer Grant No. CHE-0716718).

Supporting Information Available: Full details of the ab initio computations done in support of the spectroscopy here, including the structures, energetics and vibrational frequencies for each of the isomeric structures considered. This material is available free of charge via the Internet at http://pubs.acs.org.

References and Notes

(1) Prakash, G. K. S., Schleyer, P. v. R., Eds.; *Stable Carbocation Chemistry*; John Wiley and Sons: New York, 1997.

(2) Olah, G. A., Prakash, G. K. S., Eds.; *Carbocation Chemistry*; John Wiley and Sons: Hoboken, NJ, 2004.

(3) Holmes, J. l.; Aubrey, C.; Mayer, P. M. *Assigning Structures to Ions in Mass Spectrometry*; CRC Press: Boca Raton, FL, 2007.

(4) Glassgold, A. E.; Omont, A.; Guélin, M. *Astrophys. J.* **1992**, *396*, 115.

(5) Hartquist, T. W.; Williams, D. A. *The Molecular Astrophysics of Stars and Galaxies*; Clarendon Press: Oxford, 1998.

(6) Żurawski, B.; Ahlrichs, R.; Kutzelnigg, W. *Chem. Phys. Lett.* **1973**, *21*, 309.

(7) Lee, T. J.; Schaefer, H. F. *J. Chem. Phys.* **1986**, *85*, 3437.

(8) Lindh, R.; Roos, B. O.; Kraemer, W. P. *Chem. Phys. Lett.* **1987**, *139*, 407.

(9) Curtiss, L. A.; Pople, J. A. *J. Chem. Phys.* **1988**, *88*, 7405.

(10) Liang, C.; Hamilton, T. P.; Schaefer, H. F. *J. Chem. Phys.* **1990**, *92*, 3653.

(11) Klopper, W.; Kutzelnigg, W. *J. Phys. Chem.* **1990**, *94*, 5625.

(12) Lindh, R.; Rice, J. E.; Lee, T. J. *Chem. Phys.* **1991**, *94*, 8008.

(13) Marx, D.; Parrinello, M. *Science* **1996**, *271*, 179.

(14) Sharma, A. R.; Wu, J.; Braams, B. J.; Carter, S.; Schneider, R.; Shepler, B.; Bowman, J. M. *J. Chem. Phys.* **2006**, *125*, 224306.

(15) (a) Crofton, M. W.; Jagod, M. F.; Rehfuss, B. D.; Oka, T. *J. Chem. Phys.* **1989**, *91*, 5139. (b) Gabrys, C. M.; Uy, D.; Jagod, M.-F.; Oka, T. *J. Phys. Chem.* **1995**, *99*, 15611.

(16) Bogey, M.; Bolvin, H.; Cordonnier, M.; Demuynck, C.; Destombes, J. L. *Astrophys. J.* **1992**, *399*, L103.

(17) Bogey, M.; Bolvin, H.; Cordonnier, M.; Demuynck, C.; Destombes, J. L. *Can. J. Phys.* **1994**, *72*, 967.

(18) Cordonnier, M.; Coudert, L. H. *J. Mol. Spectrosc.* **1996**, *178*, 59.

(19) (a) Yeh, L. I.; Okumura, M.; Myers, J. D.; Price, J. M.; Lee, Y. T. *J. Chem. Phys.* **1989**, *91*, 7319−7330. (b) Okumura, M.; Yeh, L. I.; Myers, J. D.; Lee, Y. T. *J. Phys. Chem.* **1990**, *94*, 3416.

(20) Ebata, T.; Fujii, A.; Mikami, N. *Intl. Rev. Phys. Chem.* **1998**, *17*, 331.

(21) Bieske, E. J.; Dopfer, O. *Chem. Rev.* **2000**, *100*, 3963.

(22) Robertson, W. H.; Johnson, M. A. *Ann. Rev. Phys. Chem.* **2003**, *54*, 173.

(23) Duncan, M. A. *Intl. Rev. Phys. Chem.* **2003**, *22*, 407.

(24) Vager, Z.; Zajfman, D.; Graber, T.; Kanter, E. P. *Phys. Rev. Lett.* **1993**, *71*, 4319.

(25) Knoll, L.; Vager, Z.; Marx, D. *Phys. Rev. A* **2003**, *67*, 022506.

(26) Feng, W. Y.; Ling, Y.; Lifshitz, C. *J. Phys. Chem.* **1996**, *100*, 35.

(27) McMahon, T. B. *Adv. Gas Phase Ion Chem.* **1996**, *2*, 41.

(28) Ewing, R. G.; Eiceman, G. A.; Stone, J. A. *Int. J. Mass Spectrom.* **1999**, *193*, 57.

(29) Hache, J. J.; Laskin, J.; Futtrell, J. H. *J. Phys. Chem. A* **2002**, *106*, 12051.

(30) Meot-Ner, M. *Chem. Rev.* **2005**, *105*, 213.

(31) Asmis, K. R.; Pivonka, N. L.; Santambrogio, G.; Brummer, M.; Kaposta, C.; Neumark, D. M.; Wöste, L. *Science* **2003**, *299*, 1375.

(32) Fridgen, T. D.; McMahon, T. B.; MacAleese, L.; Lemaire, J.; Maitre, P. *J. Phys. Chem. A* **2004**, *108*, 9008.

(33) Headrick, J. M.; Diken, E. G.; Walters, R. S.; Hammer, N. I.; Christie, R. A.; Cui, J.; Myshakin, E. M.; Duncan, M. A.; Johnson, M. A.; Jordan, K. D. *Science* **2005**, *308*, 1765.

(34) (a) Diken, E. G.; Headrick, J. M.; Roscioli, J. R.; Bopp, J. C.; Johnson, M. A. *J. Phys. Chem. A* **2005**, *109*, 1487. (b) Hammer, N. I.; Diken, E. G.; Roscioli, J. R.; Johnson, M. A.; Myshakin, E. M.; Jordan, K. D.; McCoy, A. B.; Huang, X.; Bowman, J. M.; Carter, S. *J. Chem. Phys.* **2005**, *122*, 244301.

(35) Stoyanov, E. S.; Reed, C. A. *J. Phys. Chem. A* **2006**, *110*, 12992.

(36) (a) Huang, X.; Braams, B. J.; Bowman, J. M. *J. Chem. Phys.* **2005**, *122*, 044308. (b) Kaledin, M.; Kaledin, A. L.; Bowman, J. M. *J. Phys. Chem. A* **2006**, *110*, 2933.

(37) Stoyanov, E. S. *Phys. Chem. Chem. Phys.* **2000**, *2*, 1137.

(38) Moore, D. T.; Oomens, J.; Van Der Meer, L.; Von Helden, G.; Meijer, G.; Valle, J.; Marshall, A. G.; Eyler, J. R. *Chem. Phys. Chem*. **2004**, *5*, 740.

(39) (a) Fridgen, T. D.; MacAleese, L.; Maitre, P.; McMahon, T. B.; Boissel, P.; Lemaire, J. *Phys. Chem. Chem. Phys.* **2005**, *7*, 2747. (b) Fridgen, T. D.; MacAleese, L.; McMahon, T. B.; Lemaire, J.; Maitre, P. *Phys. Chem. Chem. Phys.* **2006**, *8*, 955.

(40) Roscioli, J. R.; McCunn, L. R.; Johnson, M. A. *Science* **2007**, *316*, 249.

(41) Qu, Z.; Zhu, H.; Ma, S.; Xu, H.; Zhang, R.; Zhang, X.; Zhang, Q. *Chem. Phys. Lett.* **2001**, *348*, 95.

(42) Grabowski, S. J.; Sokalski, W. A.; Leszczynski, J. *J. Phys. Chem. A* **2004**, *108*, 1806.

(43) Frisch, M. J.; Trucks, G. W.; Schlegel, H. B.; Scuseria, G. E.; Robb, M. A.; Cheeseman, J. R.; Montgomery, J. A., Jr.; Vreven, T.; Kudin, K. N.; Burant, J. C.; Millam, J. M.; Iyengar, S. S.; Tomasi, J.; Barone, V.; Mennucci, B.; Cossi, M.; Scalmani, G.; Rega, N.; Petersson, G. A.; Nakatsuji, H'Hada, M.; Ehara, M.; Toyata, K.; Fukuda, R.; Hasegawa, J.; Ishida, M.; Nakajima, T.; Honda, Y.; Kitao, O.; Nakai, H.; Klene, M.; Li, X.; Knox, J. E.; Hratchian, H. P.; Cross, J. B.; Adamo, C.; Jaramillo, J.; Gomperts, R.; Stratmann, R. E.; Yazyev, O.; Austin, A. J.; Cammi, R.; Pomelli, C.; Ochterski, J. W.; Ayala, P. Y.; Morokuma, K.; Voth, G. A.; Salvador, P.; Dannenberg, J. J.; Zakrzewski, V. G.; Dapprich, S.; Daniels, A. D.; Strain, M. C.; Farkas, O.; Malick, D. K.; Rabuck, A. D.; Raghavachari, K.; Foresman, J. B.; Ortiz, J. V.; Cui, Q.; Baboul, A. G.; Clifford, S.; Cioslowski, J.; Stefanov, B. B.; Liu, G.; Liashenko, A.; Piskorz, P.; Komaromi, I.; Martin, R. L.; Fox, D. J.; Keith, T.; Al-Laham, M. A.; Peng, C. Y.; Nanayakkara, A.; Challacombe, M.; Gill, P. M. W.; Johnson, B.; Chen. W.; Wong, M. W.; Gonzalez, C.; Pople, J. A. *Gaussian 03*, revision B.02; Gaussian, Inc.: Pittsburgh, PA, 2003.

(44) (a) Schmidt, M. W.; Baldridge, K. K.; Boatz, J. A.; Elbert, S. T.; Gordon, M. S.; Jensen, J. H.; Koseki, S.; Matsunaga, N.; Nguyen, K. A.; Su, S.; Windus, T. L.; Dupuis, M.; Montgomery, J. A. *J. Comput. Chem.* **1993**, *14*, 1347. (b) Gordon, M. S.; Schmidt, M. W. In *Theory and Applications of Computational Chemistry: The First Forty Years*; Dykstra, C. E., Frenking, G., Kim, K. S., Scuseria, G. E., Eds.; Elsevier: Amsterdam, 2005; p 1167.

(45) Scott, A. P.; Radom, L. *J. Phys. Chem.* **1996**, *100*, 16502.

(46) Shimanouchi, T. *Molecular Vibrational Frequencies*; NIST Chemistry WebBook, NIST Standard Reference Database Number 69; Linstrom, P. J., Mallard, W. G., Eds.; National Institute of Standards and Technology: Gaithersburg, MD, 2005; http://webbook.nist.gov.

(47) Begeman, M. H.; Gudeman, C. S.; Pfaff, J.; Saykally, R. J. *Phys. Rev. Lett.* **1983**, *51*, 554.

(48) Dopfer, O.; Olkhov, R. V.; Roth, D.; Maier, J. P. *Chem. Phys. Lett.* **1998**, *296*, 585.

(49) Douberly, G. E.; Ricks, A. M.; Ticknor, B. W.; Duncan, M. A. *J. Phys. Chem. A* **2008**, *112*, 950.

(50) Douberly, G. E.; Ricks, A. M.; Ticknor, B. W.; Duncan, M. A. *Phys. Chem. Chem. Phys.* **2008**, *10*, 77.

(51) Douberly, G. E.; Ricks, A. M.; Ticknor, B. W.; Schleyer, P. v. R.; Duncan, M. A. work in progress.

(52) Hunter, E. P.; Lias, S. G. "Proton Affinity Evaluation," *NIST Chemistry WebBook*, NIST Standard Reference Database Number 69; National Institute of Standards and Technology: Gaithersburg, MD, 2005; http://webbook.nist.gov.

(53) Cunje, A.; Rodriguez, C. F.; Lien, M. H.; Hopkinson, A. C. *J. Org. Chem.* **1996**, *61*, 5212.

(54) Valtazanos, P.; Ruedenberg, K. *Theor. Chim. Acta* **1986**, *69*, 281.

(55) Douberly, G. E.; Ricks, A. M.; Ticknor, B. W.; Schleyer, P. v. R.; Duncan, M. A. *J. Am. Chem. Soc.* **2007**, *129*, 13782.

(56) Walters, R. S.; Jaeger, T. D.; Duncan, M. A. *J. Phys. Chem. A* **2002**, *106*, 10482.

(57) Momoh, P. O.; Abrash, S. A.; Mabrouki, R.; El-Shall, M. S. *J. Am. Chem. Soc.* **2006**, *128*, 12408.

(58) Douberly, G. E.; Ricks, A. M.; Schleyer, P. v. R.; Duncan, M. A. to be submitted.